

This is the final peer-reviewed accepted manuscript of:

Li, Weixing, Imanol Usabiaga, Camilla Calabrese, Luca Evangelisti, Assimo Maris, Laura B. Favero, and Sonia Melandri. "Characterizing the lone pair... π -hole interaction in complexes of ammonia with perfluorinated arenes." *Physical Chemistry Chemical Physics* 23, no. 15 (2021): 9121-9129.

The final published version is available online at:
<https://doi.org/10.1039/D1CP00451D>



Rights / License:

The terms and conditions for the reuse of this version of the manuscript are specified in the publishing policy. For all terms of use and more information see the publisher's website.

This item was downloaded from IRIS Università di Bologna (<https://cris.unibo.it/>)

When citing, please refer to the published version.

Characterizing the lone pair $\cdots \pi$ -hole interaction in complexes of ammonia with perfluorinated arenes†

Weixing Li, ^{‡§a} Imanol Usabiaga, ^{‡a} Camilla Calabrese, ^{★bcd}
Luca Evangelisti, ^a Assimo Maris, ^a Laura B. Favero ^e and Sonia Melandri ^{★a}

When hydrogen is completely replaced by fluorine, arenes become prone to forming a lone pair $\cdots \pi$ -hole non-covalent bond with ligands presenting electron rich regions. Such a species is ammonia, which confirms this behavior engaging its lone pair as the electron donor counterpart in the 1:1 adducts with hexafluorobenzene and pentafluoropyridine. In this work, the geometrical parameters of the interaction have been unambiguously identified through the detection, by means of Fourier transform microwave spectroscopy, of the rotational spectra of both normal species and their $^{15}\text{NH}_3$ isotopologues. An accurate analysis of the experimental data, including internal dynamics effects, endorsed by quantum chemical calculations, both with topological analysis and energy decomposition method, extended to the hydrogenated arenes and their water complexes, proved the ability of ammonia to create a stronger and more flexible lone pair $\cdots \pi$ -hole interaction than water. Interestingly, the higher binding energies of the ammonia lone pair $\cdots \pi$ -hole interactions correspond to larger intermolecular distances.

Received 31st January 2021,
Accepted 22nd March 2021

DOI: 10.1039/d1cp00451d

rsc.li/pccp

Introduction

Non-covalent interactions (NCIs) play a very important role in many physical, chemical and biochemical processes and the interest in their experimental and theoretical characterization is testified by the large amount of literature on this theme.^{1–4} Among NCIs, the hydrogen bond (HB) is recognized to be the most diffuse and important one and its discovery is now one century old.^{5–7} In recent years, other kinds of intermolecular interactions involving different atoms or fragments that can replace the bridging proton of the HB and attract an electron donor *via* a region of depleted electron density, have been a subject of great interest. This region is called a “hole” and,

depending on whether it is in the direction of or perpendicular to the molecular σ -framework, it is called a “ σ ”- or a “ π -hole”, respectively. The formation of a “hole” can be obtained by suitable substitutions.^{8–10} It is known that halogen atoms, fluorine in particular, can drastically change the interaction properties of molecules; therefore, fluorine substitution is used to tune the features of new materials,¹¹ drugs^{12,13} or proteins.¹⁴ The effect of fluorine substitution in peptides for example, has been shown to impart favourable but not easily predictable properties.¹⁵

Incorporating the C–F bond into a molecule can give rise to different phenomena: the fluorine atom can directly engage in intermolecular interactions with its environment but also influence, through its electron withdrawing effect, other functional groups in the same molecule, which will then interact differently with their immediate environment. In this sense, the action exerted by fluorine on the binding abilities of a molecule perfectly represents a “through-space” substitution effect. Actually, the effect generated by the sequential addition of fluorine atoms on the electron density is a shift of the electronic cloud towards the halogen atom causing the formation of a “hole” of diminished electron density.^{16–18} Interestingly, the through-space substitution effects prevail over the through-bond ones in arene π -systems,¹⁹ for which NCIs are extremely important in all fields of chemistry and biochemistry.²⁰ For these reasons, it seemed particularly interesting to study the influence of full fluorination

^a Department of Chemistry “Giacomo Ciamician”, University of Bologna, via Selmi, 2, 40126, Bologna, Italy. E-mail: sonia.melandri@unibo.it

^b Department of Physical Chemistry, University of the Basque Country (UPV/EHU), Barrio Sarriena, S/N, 48940, Leioa, Spain. E-mail: calabrese.cami@gmail.com

^c Biofisika Institute, (CSIC, UPV/EHU), Barrio Sarriena, S/N, 48940, Leioa, Spain

^d Fundación Biofisika Bizkaia/Biofisika Bizkaia Fundazioa (FBB), Barrio Sarriena, S/N, 48940, Leioa, Spain

^e Istituto per lo studio dei materiali nanostrutturati CNR – ISMN, Via Gobetti 101, 40129, Bologna, Italy

† Electronic supplementary information (ESI) available: Theoretical equilibrium structures; survey scan; experimental transition frequencies; experimental Ssecroscopic parameters; substitution structures. See DOI: 10.1039/d1cp00451d

‡ These authors contributed equally to this work.

§ Present address: Department of Chemistry, Fudan University, Shanghai 200438, China.

(perfluorination) on the binding properties of aromatic rings such as benzene and pyridine.

Hexafluorobenzene (C_6F_6) and pentafluoropyridine (C_5F_5N) were chosen as prototype perfluorinated aromatic systems and cavity-based Fourier transform microwave (FTMW) spectroscopy performed in a supersonic expansion was selected as the investigation tool. The high resolution and sensitivity of the experimental technique allow the accurate determination of the interaction in the absence of solvent and matrix effects. Using this experimental technique, unique information can be obtained: in particular highly detailed structural parameters and dynamical information related to internal motions both in molecules^{21,22} and non-covalently bound complexes.^{23,24}

Rotational spectroscopy investigations of the 1 : 1 adducts of hydrogenated and perfluorinated arenes with water have been performed recently. In both the gas phase complexes $C_6F_6 \cdot W$ ²⁵ and $C_5F_5N \cdot W$ ²⁶ (here W represents the water molecule), the water molecule lies above the aromatic plane with the oxygen lone-pairs pointing towards what has been characterized as a π -hole at the center of the ring and thus forming the lone pair $\cdots \pi$ -hole interaction (from now on indicated as lp $\cdots \pi$ -hole). The determined orientation of the water molecule in $C_6F_6 \cdot W$ is opposite to that observed in the complex with benzene ($C_6H_6 \cdot W$),²⁷ where, although a complex dynamical situation is present, the evidence is that the water molecule forms an O-H $\cdots \pi$ HB with the aromatic cloud of benzene.

Differently, in the complex with pyridine ($C_5H_5N \cdot W$),²⁸ the presence of the nitrogen atom allows for the formation of a relatively strong in-plane O-H $\cdots N$ HB with water, which becomes weaker and is overcome by the new lp $\cdots \pi$ -hole interaction in the perfluorinated analogue ($C_5F_5N \cdot W$).²⁶ These results can be considered as direct evidence of the effect of perfluorination on the aromatic cloud of benzene and pyridine and show that in perfluorinated aromatic compounds the "hole" is formed perpendicularly to the bond frame (π -hole) differently from that, which is formed along the bond (σ -hole).^{9,29}

As indicated by these previous results, fluorine is very effective in tuning the binding properties of aromatic rings; nevertheless, the outcome is not easily predictable. When only one or two fluorine atoms are present as substituents in the aromatic ring, the lp $\cdots \pi$ -hole interaction is not observed. In fact, in the water complexes of fluorobenzene and *p*-difluorobenzene³⁰ the water molecule is bound in-plane forming a HB to the fluorine atom and also in the complexes of 2- and 3-fluoropyridine with water,^{31,32} the water molecule maintains the in-plane O-H $\cdots N$ HB shown in the $C_5H_5N \cdot W$ complex. Preliminary results obtained in our laboratory indicate that the in-plane interaction prevails in fluorine-substituted pyridine-water complexes even if four out of five hydrogen atoms are substituted.³³ Intrigued by these results and eager to investigate further, we have undertaken, and we report here, the rotational spectroscopy investigation of complexes formed by C_6F_6 and C_5F_5N with another prototype polar ligand: ammonia.

Ammonia, although possessing a N-H bond, is known, differently from water, to be an almost universal proton

acceptor even with the weakest donors.³⁴ Nevertheless, it has been shown to form HBs, although generally much weaker than those formed by water.^{35–37} In particular, it behaves similarly to water in binding to benzene with a NH $\cdots \pi$ HB³⁸ and in forming an in-plane N-H $\cdots N$ HB with the heteroaromatic nitrogen atom of pyridine.³⁹ Also, it has been found that ammonia gives rise to lp $\cdots \pi$ -hole interactions with fluorine substituted ethylene.¹⁷

The fact that ammonia presents a single lone pair gives it interesting properties if compared to water. In fact, in water complexes the simultaneous interaction of the two lone pairs of the oxygen atom usually prevails over a centered interaction of a single lone pair. We thought it interesting to relate this feature with the structure and the binding energies of the 1 : 1 complexes, and in turn understand the effect produced on the dynamics and the intermolecular interaction by the insertion of a heteroatom such as in C_5F_5N as we will show in the following.

Results and discussion

Quantum chemical calculations, performed at the B3LYP-GD3(BJ)/def2-TZVP level using the GAUSSIAN16 software package,⁴⁰ suggest that in the global minimum structure of both complexes, $C_6F_6 \cdot NH_3$ and $C_5F_5N \cdot NH_3$, the ammonia molecule lies above the aromatic plane, pointing its nitrogen lone pair towards the centre of the ring. For $C_5F_5N \cdot NH_3$ a second conformation where the N-H bond points toward the ring has been optimized but its stabilization electronic energy is much higher (10.6 kJ mol⁻¹). The method and basis set were chosen as they proved to be accurate for the structural characterization of molecular complexes also when dispersion terms are important in shaping the conformational space.⁴¹

According to the geometries shown in Fig. 1, the symmetry axes of ammonia and C_6F_6 are coincident, leading to the C_{3v} symmetry, whereas when interacting with C_5F_5N , the ligand slightly bends toward the pyridinic nitrogen leading to the C_s symmetry. $C_6F_6 \cdot NH_3$ can thus be classified as an oblate symmetric rotor characterized by the rotational constant $B = 766.3$ MHz, the electric dipole moment lying along the symmetry axis $\mu_c = 2.15$ D and the nuclear quadrupole coupling constant (responsible for the coupling of the nuclear quadrupole moment to the overall molecular rotation) $\chi_{cc} = -4.43$ MHz. On the other hand, $C_5F_5N \cdot NH_3$ is predicted to give rise to the rotational spectrum of an asymmetric rotor with sizeable values of both μ_b and μ_c dipole moment components. The depiction of the equilibrium structures for both systems together with the calculated structural parameters of $C_5F_5N \cdot NH_3$ can be found in the ESI† (Tables S1–S3).

Guided by the theoretical predictions, the rotational spectra of $C_6F_6 \cdot NH_3$ and $C_5F_5N \cdot NH_3$ were recorded in the 6–18 GHz range with FTMW spectroscopy using the instrument and the conditions described in the Experimental section. In agreement with the predictions, the rotational spectrum observed for the $C_6F_6 \cdot NH_3$ system was indeed that of a symmetric rotor and several progressions $J + 1 \leftarrow J$ with rotational quantum number J

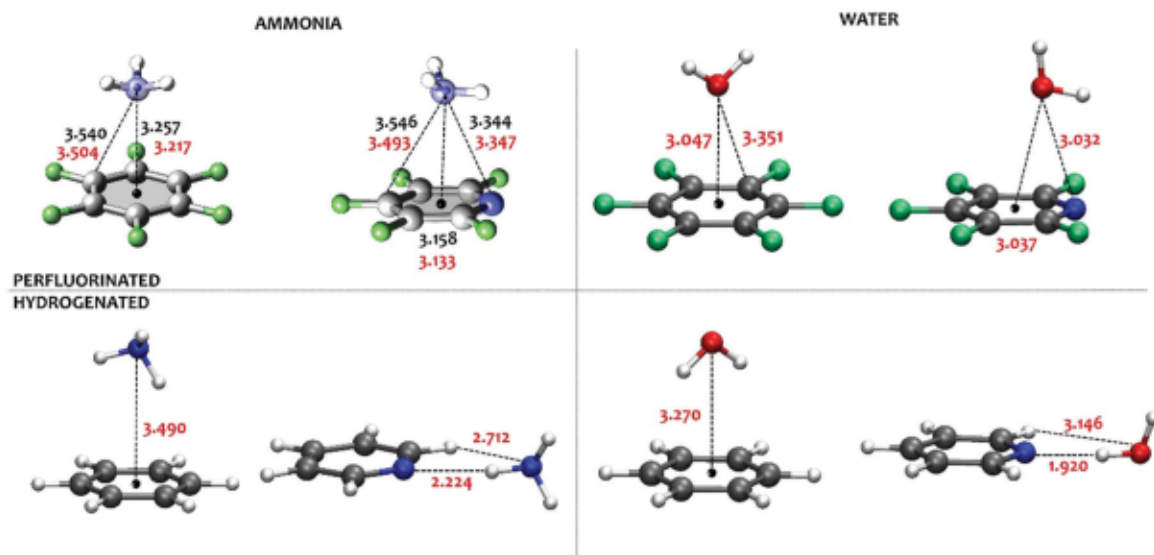


Fig. 1 Molecular structure and intermolecular distances (in Å) for $C_6F_6 \cdot W \cdot NH_3$ and $C_5F_5N \cdot W \cdot NH_3$, $C_6H_6 \cdot W \cdot NH_3$ and $C_5H_5N \cdot W \cdot NH_3$. Ball and stick representation and red values from B3LYP-GD3(BJ)/def2-TZVP calculations. Superimposed small blue spheres and black values from experimental substitution coordinates (only for $C_6F_6 \cdot NH_3$ and $C_5F_5N \cdot NH_3$).

ranging from 4 to 8 were identified. The observed band features (see Fig. 2) suggest an almost free rotation of the ammonia moiety analogous to that observed for $C_6H_6 \cdot W$ and $C_6F_6 \cdot W$. Considering the NH_3 molecules as the rotating top and C_6F_6 as the framework, the internal rotational state of the complex is specified by the quantum number m , the projection of the angular momentum of the NH_3 unit on the symmetry axis of the complex.

Both the $^{14}NH_3$ and the $^{15}NH_3$ complexes were investigated; in the case of the former one, additional nuclear quadrupole coupling splitting, arising from the coupling of the nuclear quadrupole moment ($I(N) = 1$ for $^{14}NH_3$) and ($I(N) = 0$ for $^{15}NH_3$) to the overall rotation of the molecular species, were observed leading to a very complex hyperfine spectral structure. The rotational transitions have been satisfactorily fitted with

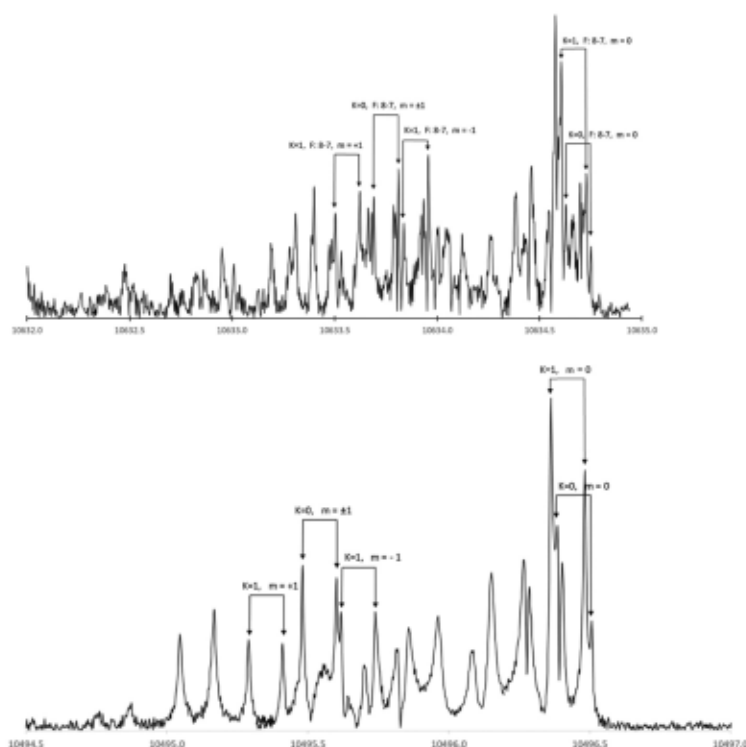


Fig. 2 Survey scan (MHz) for the $J: 7 \leftarrow 6$ transition of $C_6F_6 \cdot ^{14}NH_3$ (top) and $C_6F_6 \cdot ^{15}NH_3$ (bottom).

the equation reported below⁴² to which, for the $C_6F_6\cdot^{14}NH_3$ case, the standard nuclear quadrupole term for the symmetric top was added.⁴³

$$\nu(J+1 \leftarrow J) = 2B(J+1) - 4D_J(J+1)^3 - 2D_{JK}(J+1) \cdot K^2 - 2H_{KJ}(J+1) \cdot K^4 - 2D_{Jm}(J+1) \cdot m^2 - 2D_{JKm}(J+1) \cdot K \cdot m + f(I, J, F, K) \cdot \chi_{cc}$$

In this expression D_J , D_{JK} , H_{KJ} , D_{Jm} and D_{JKm} are the centrifugal distortion constants, while χ_{cc} is the nuclear quadrupole constant for the nitrogen atom along the c inertial axis. The coupling scheme used for the labelling of the rotational transitions is: $F_1 = I_1 + J$ and $F = I_2 + F_1$ with J being the rotational quantum number and I_1 and I_2 the nuclear quadrupole moments of the two nitrogen atoms. All fitted transitions are reported in the ESI† (Tables S4 and S5) and the resulting spectroscopic parameters for both isotopologues are reported in Table 1.

As regards the experimental nuclear quadrupole coupling constant along the c axis ($\chi_{cc} = -3.17(2)$ MHz), it is smaller than the calculated one ($\chi_{cc} = -4.43$ MHz), which in turn is slightly larger than that of free ammonia ($\chi_{cc} = -4.089$ MHz),⁴⁴ but it is very similar to the corresponding value observed in other ammonia complexes.⁴⁵ These differences have been attributed to large amplitude motions of the ammonia moiety with respect to the inertial axis.⁴⁶ Concerning $C_5F_5N \cdot NH_3$, the spectrum observed was that of an asymmetric top. Several progressions $J+1 \leftarrow J$ with rotational quantum number J ranging from 4 to 7 and pseudo quantum number K_c from 0 to 7 have been observed and analysed for both the normal and the $C_5F_5N \cdot ^{15}NH_3$ species. The normal species presents two nitrogen nuclei that contribute to the nuclear hyperfine structure observed in the spectrum, while in the $C_5F_5N \cdot ^{15}NH_3$ complex, only the hyperfine structure related to the aromatic nitrogen atom is observed. The measured rotational transitions were fitted using the SPFIT program⁴⁷ within the I' representation of Watson's S reduction.⁴⁸ All transitions are reported in the ESI† (Tables S6 and S7), while the fitted spectroscopic parameters are reported in Table 2. The deviation between the experimental and calculated rotational constants (lower energy conformer) is less than 1%, confirming the assignment.

Analysis of the rotational constants of the isotopologues, which differ because of the different masses, allows the deduction of structural parameters for the substituted atoms. From the two

Table 2 Experimental spectroscopic parameters of $C_5F_5N \cdot NH_3$

	$C_5F_5N \cdot ^{14}NH_3$	$C_5F_5N \cdot ^{15}NH_3$
A /MHz	996.25781(9) ^a	980.2763(1)
B /MHz	803.41525(8)	793.8382(1)
C /MHz	618.2949(2)	617.8025(6)
D_J /kHz	0.242(1)	[0.242] ^b
D_{JK} /kHz	0.685(3)	[0.685]
D_K /kHz	-0.717(3)	[-0.717]
d_1 /kHz	-0.0208(9)	[-0.0208]
d_2 /kHz	0.0865(3)	[0.0865]
$\chi_{aa}(C_5F_5N)$ /MHz	1.967(4)	1.967(7)
$\chi_{bb}-\chi_{cc}(C_5F_5N)$ /MHz	-5.583(4)	-5.548(8)
$\chi_{aa}(NH_3)$ /MHz	1.631(4)	—
$\chi_{bb}-\chi_{cc}(NH_3)$ /MHz	2.803(4)	—
N^c	390	71
σ /kHz ^d	2.6	3.5
$\mu_a/\mu_b/\mu_c$	No/yes/yes	No/yes/yes

^a Standard error in parentheses in units of the last digit. ^b In brackets, values fixed to those determined for the normal species. ^c Number of lines in the fit. ^d Root-mean-square deviation of the fit.

sets of rotational constants determined for each complex using normal NH_3 or $^{15}NH_3$, the substitution coordinates (r_s) of the ammonia nitrogen atom can be obtained by applying Kraitichman's equations.⁴⁹ The use of these relations is based on the standard assumption of the isotopic invariance of molecular geometries and does not require any *a priori* assumption. In the ESI† (Table S8) the values of the r_s coordinates are reported, while in Fig. 1 the experimental partial r_s structure is superimposed on the theoretical equilibrium one. The comparison of these data further confirms the assignment of the observed spectra and allows estimating the accuracy of the theoretical calculations. Looking closer at Fig. 1, we can see that the structural arrangements are in good agreement and the differences between the calculated interatomic distances and those estimated from the r_s in the studied systems do not exceed 60 mÅ. These observations allow us to rely on the theoretical properties for a comparison and generalization of the behaviour of hydrogenated and perfluorinated arenes with water and ammonia.

To do so, the structures of the water complexes of hexafluorobenzene and pentafluoropyridine together with the ammonia and water complexes of their hydrogenated counterparts, benzene and pyridine, have been characterized with the same method and basis set. For these systems, a systematic comparison between calculated and experimentally derived structures is difficult because the data are not always reported in the literature, but the authors have verified that the calculated structures yield rotational constants, which differ from the experimental ones within 4% at this level of calculation. This proves the reliability of the quantum chemical calculations for what concerns their ability to model all the interactions and allows the comparisons among the different systems based on the calculated values of distances and energies. The theoretical data (see Fig. 1 where the calculated distances for all systems are reported) show that in the HBs established with pyridine, the weaker ability of ammonia to form these interactions with respect to water is reflected by the larger interaction distance observed in the ammonia complexes ($N-H \cdots N = 2.224$ Å in $C_5H_5N \cdot NH_3$ and

Table 1 Experimental spectroscopic parameters of $C_6F_6 \cdot NH_3$

	$C_6F_6 \cdot ^{14}NH_3$	$C_6F_6 \cdot ^{15}NH_3$
B /MHz	759.6291(1) ^a	749.7555(2)
D_J /kHz	0.0910(7)	0.093(2)
D_{JK} /kHz	1.899(7)	1.94(1)
H_{KJ} /Hz	-4.3(2)	-3.3(3)
D_{Jm} /kHz	67.01(5)	64.9(1)
D_{JKm} /kHz	11.178(1)	11.177(3)
χ_{cc} /MHz	-3.17(2)	—
N^b	157	44
σ^c /kHz	3.2	3.9

^a Standard error in parentheses in units of the last digit. ^b Number of lines in the fit. ^c Root-mean-square deviation of the fit.

O-H...N = 1.920 Å in C₅F₅N-W). This is also observed in the case of the benzene complexes, in which the ammonia and water molecules interact *via* a weak HB to the π -cloud and again ammonia appears to be more distant than water (3.490 Å vs. 3.270 Å). In the lp... π -hole complexes formed by the perfluorinated moieties, the distance of the water oxygen or the ammonia nitrogen to the centre of the ring ranges from 3.037 Å in C₅F₅N-W to 3.217 Å in C₆F₆·NH₃. The distance is larger for the ammonia complexes with respect to those with water and in the ones involving C₆F₆ with respect to those with C₅F₅N.

A deeper analysis of the potential energy as a function of the orientation of the ligands was also undertaken. In Fig. 3 the shape of the potential energy functions for the internal rotation of the two ligands (water and ammonia) around the C₂ or C₃ axis in C₆F₆·W, ·NH₃, and C₅F₅N·W, ·NH₃ are shown. They are obtained using the B3LYP-GD3(BJ)/def2-TZVP level of theory and the internal rotation coordinate is moved with a step size of 5°, while all the other geometrical parameters were freely optimized.

The picture, which we can infer from these results, is that in the complexes with C₆F₆, and in the minimum of the curve, the C₂ or C₃ symmetry axis of water or ammonia, respectively, is perfectly aligned with the axis normal to the plane of the ring and centred in the π -hole. This does not prevent the NH₃ molecule from undergoing an almost free rotation around its axis and a wagging motion responsible for the value of χ_{cc} being smaller than the theoretical one. Moreover, in both cases the resulting V₆ barrier is dictated by the aromatic ring, giving rise to an almost inexistent gap (about 0.02 kJ mol⁻¹). This factor, together with the relatively light mass of the hydrogen atoms, indicates that the ligands can be considered completely delocalized with respect to the symmetry axis, which causes the systems to be effectively symmetric tops, in agreement with the experimental observations. The insertion of a perturbing heteroatom in the ring, the nitrogen, causes a shift in the ligand position, thus the corresponding lone pairs are now unable to interact symmetrically with the π -hole. This fact produces an eccentric rotation of water or ammonia that is responsible for the surging of a barrier. The barrier to the

rotation of the ligand represents ~9% of destabilization for C₅F₅N-W and less than 2% for C₅F₅N-NH₃.

To visualize and quantify the interactions and their energies, the topology of the theoretical electron densities was analysed with the Multiwfn program,⁵⁰ which is based on the atoms in molecules theory (AIM).⁵¹ Complementary information was also achieved visualizing the interactions with the NCI method,⁵² which considers the distribution of both the electron density and its gradient. A comprehensive picture can be drawn using these regions of density overlap for both the hydrogenated and perfluorinated arenes with ammonia and water. An advantage of this method is that the NCI index has proved to be very little dependent on the method and basis set used in the calculation once the geometry is fixed.⁵³ The isosurfaces visible in the NCI plots are reported in Fig. 4 and according to the colour code reported on the graphs, they represent the areas for attractive and repulsive interactions.

In Fig. 4, the lp... π -hole attractive interactions present in the water and ammonia complexes with both C₆F₆ and C₅F₅N can be easily viewed. In the case of the C₆F₆ complexes, the structure of the interaction region is perfectly symmetrical with respect to an axis normal to the ring plane and passing through its centre, while a slight distortion and attractive region towards the nitrogen atom is present in the complexes of C₅F₅N. Despite this, it is clearly visible that the shape of the interaction, which represents the lp... π -hole (small green circle) is more symmetric for ammonia than for water, giving further proof of the greater directionality of the ammonia lp... π -hole interaction. For comparison, in the complexes of the hydrogenated arenes these interactions are replaced by HBs to the π -cloud (OH, and NH... π) for C₆H₆·W and C₆H₆·NH₃ or to the heterocyclic nitrogen (OH, and NH...N) in C₅H₅N·W and C₅H₅N·NH₃, respectively.

In order to understand if, as observed in the HB systems, the trend of the distances is in any relation with the energies involved in the interactions, a quantitative understanding of the chemical nature of the NCIs has been achieved by an energy decomposition analysis, using the symmetry-adapted perturbation theory.⁵⁴ Using this scheme and methodology, the energy of the intermolecular interaction can be interpreted as the sum of different terms with a defined physical meaning: electrostatic, induction, dispersion and exchange-repulsion terms. The SAPT analysis has been carried out using the PSI4 package⁵⁵ at the SAPT2+3(CCD)/aug-cc-pVDZ level on the same group of complexes and the results are summarized in Table 3. In the same table the binding energies (*B_e*) calculated at the B3LYP-GD3(BJ)/def2-TZVP level are also reported. The agreement of *B_e* with the SAPT total energies is very good for the complexes held by the lp... π -hole interaction, while the SAPT calculations are systematically smaller for the systems bound by a HB. In general, the SAPT values are lower than the B3LYP ones but the relative energy scale is the same for both methods allowing a general discussion on the driving forces of the different interactions.

Looking at the complete set of complexes, we can see that the in-plane HB of C₅H₅N·W stands out for having a total energy at least one third higher than those of all the other

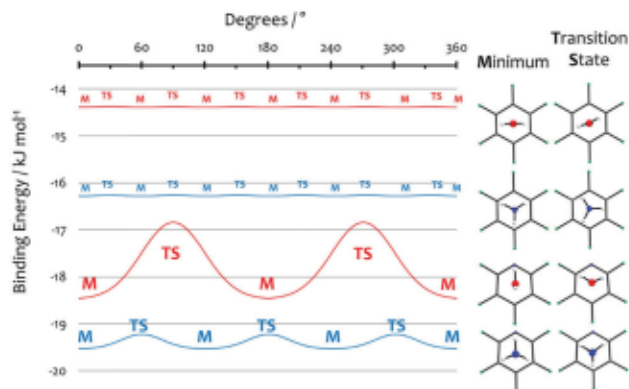


Fig. 3 The effect of the internal rotation of the ligands (ammonia or water) on the binding energy of the corresponding perfluorinated benzene (first two traces) and pyridine (last two traces) complexes.

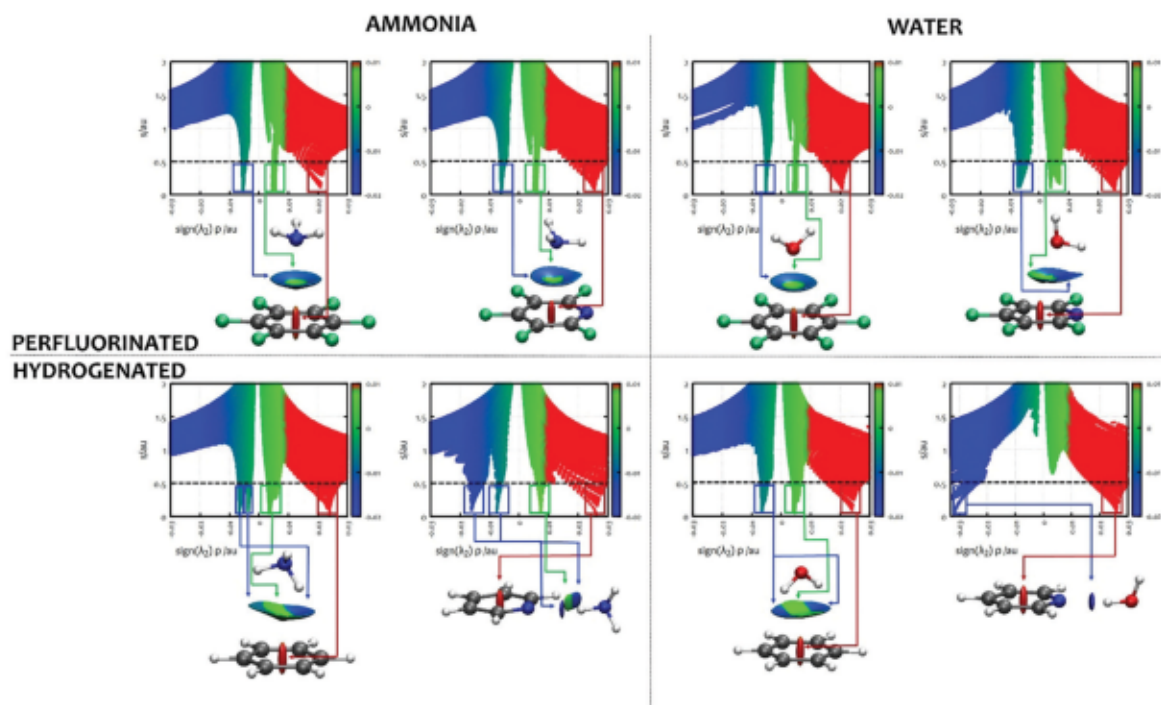


Fig. 4 The NCI plots from the theoretical (B3LYP-GD3(BJ)/def2-TZVP) electron densities of $C_6F_6 \cdots NH_3$, $C_6H_6 \cdots NH_3$, $C_5F_5N \cdots NH_3$ and $C_5H_5N \cdots W$. For each system: in the pictures the blue and green colours identify the presence of strong and weak attractive interactions, respectively, while red colour indicates repulsive interaction. The top diagrams show the value of the electron density gradient (s) vs. the electron density (ρ) multiplied by the sign of its second derivative λ_2 . Positive values indicate repulsive interactions and negative values attractive ones.

Table 3 SAPT2+3(CCD)/aug-cc-pVDZ analysis for the complexes of water and ammonia formed with C_6F_6 , C_5F_5N , C_6H_6 and C_5H_5N . The total SAPT interaction energy is compared to the density functional (B3LYP-GD3(BJ)/def2-TZVP) binding energy (B_e) (all values are in kJ mol^{-1})

Energies	Electrostatic	Induction	Dispersion	Exchange	Total	B_e
lp$\cdots\pi$-hole systems						
$C_6F_6 \cdots NH_3$	-16.03	-3.10	-13.40	17.59	-14.94	-16.26
$C_6F_6 \cdots H_2O$	-12.42	-2.67	-11.23	13.52	-12.80	-14.39
$C_5F_5N \cdots NH_3$	-20.90	-3.60	-14.90	21.22	-18.18	-19.53
$C_5F_5N \cdots H_2O$	-17.19	-3.21	-13.14	17.51	-16.03	-18.47
HB systems						
$C_6H_6 \cdots NH_3$	-8.40	-2.37	-12.73	15.19	-8.31	-11.79
$C_6H_6 \cdots H_2O$	-13.84	-4.37	-14.28	20.75	-11.74	-19.28
$C_5H_5N \cdots NH_3$	-26.97	-7.42	-13.48	31.05	-16.82	-20.06
$C_5H_5N \cdots H_2O$	-51.04	-19.26	-16.53	59.34	-27.49	-33.87

complexes that involve the π -cloud/ π -hole interaction, due to the dominant electrostatic component. The interaction is weaker for ammonia in all its HB complexes, which show a much lower interaction energy than those of their water homologues: $B_e = 20.06 \text{ kJ mol}^{-1}$ for $C_5H_5N \cdots NH_3$ compared to $B_e = 33.87 \text{ kJ mol}^{-1}$ for $C_5H_5N \cdots W$ and $B_e = 11.79 \text{ kJ mol}^{-1}$ for $C_6H_6 \cdots NH_3$ compared to $B_e = 19.28 \text{ kJ mol}^{-1}$ for $C_6H_6 \cdots W$. Indeed, the ammonia complex with benzene ($C_6H_6 \cdots NH_3$) turns out to be the least strongly bound complex, highlighting the lower interaction force exerted by the π -cloud \cdots H-N bond not only compared to the same weak HB established by water in $C_6H_6 \cdots W$, but also with respect to the lp $\cdots\pi$ -hole interaction in $C_6F_6 \cdots NH_3$. The SAPT analysis also highlights the nature of the

HB interaction. In all the HB systems the dispersion terms show similar values (from $-16.53 \text{ kJ mol}^{-1}$ for $C_5H_5N \cdots W$ to $-12.73 \text{ kJ mol}^{-1}$ for $C_6H_6 \cdots NH_3$), while the electrostatic and induction terms are larger for the pyridine complexes and decrease in the benzene ones. The electrostatic term becomes comparable (in $C_6H_6 \cdots W$) or smaller (in $C_6H_6 \cdots NH_3$) with respect to the dispersion term when the weak HB to the π -cloud is established.

Focusing on the lp $\cdots\pi$ -hole systems, it is interesting to note that whilst the electrostatic term is the largest one for all complexes, the dispersion terms are of comparable value to it, the maximum difference between the two terms being only 6 kJ mol^{-1} shown by $C_5F_5N \cdots NH_3$. In fact, as already observed by

Evangelisti *et al.*,²⁵ the electrostatic interaction, albeit smaller, represents the principal attractive term in the complexes formed by the perfluorinated compounds. In addition, it is observed that in the perfluorinated complexes all terms are slightly higher for ammonia than for the water complexes, resulting in general a slightly higher stabilization energy, which is contrary to the HB systems where water is more competitive than ammonia to interact with its partners. Since, different to what happens in HB systems, this higher binding energy is accompanied by larger distances between the moieties, we have also performed a SAPT calculation of the energy components as a function of the intermolecular distance to deepen our understanding of the driving forces of this process. We have limited the calculations to the symmetric cases of $C_6H_6 \cdots W$ and $C_6H_6 \cdots NH_3$. The results are reported in the ESI† (Fig. S1) and they clearly show that all energy contributions are larger for ammonia with respect to water at all values of the distance. This also includes the repulsive contribution, which shows the largest difference between ammonia and water at comparable distances of the ligands in the complexes. The positions of the minima are correctly reproduced with the SAPT method showing that the equilibrium position is reached for ammonia at a larger distance and higher stabilization energy than for water. So, if the ability of ammonia to form weaker HBs when compared to water is well documented,⁵⁶ with this study we can conclude that in the case of the $lp \cdots \pi$ -hole interaction the binding energy is slightly higher for ammonia with respect to water and this is probably related to the fact that the single lone pair of ammonia is able to create a more direct interaction with the π -hole than water is, with the two lone pairs straddling it.

Experimental

The rotational spectra were recorded with a COBRA-type⁵⁷ pulsed supersonic-jet Fourier-transform microwave spectrometer⁵⁸ described previously.^{59,60}

For the measurements, commercial samples of C_6F_6 , C_5F_5N (bought from Alfa Aesar), NH_3 and $^{15}NH_3$ (bought from Aldrich, anhydrous 99.9%) were used without further purification. For both $C_6F_6 \cdots NH_3$ and $C_5F_5N \cdots NH_3$ complexes, a gas mixture of NH_3 in He (a concentration of about 1–2% and a pressure of 0.3 MPa) was flowed over the liquid samples maintained at 273 K. The final mixtures were then expanded through a solenoid valve (General Valve, Series 9, and nozzle diameter 0.5 mm) into the Fabry–Perot cavity.

An alternative method was tested. It consisted in preparing a tank, which contained C_5F_5N and NH_3 in He at a concentration of 1% and a final pressure of 0.6 MPa. The mixture was then expanded into the cavity under the same conditions. This method gave similar results and no increase in the signal intensity, so the previous method was used for all the measurements.

Each rotational transition is split by the Doppler effect, mainly due to the molecular beam expansion in the coaxial arrangement of the supersonic jet and resonator axes. The rest frequency is evaluated as the arithmetic mean of the

frequencies of the Doppler components. The estimated accuracy of frequency measurements is better than 3 kHz and transitions separated by more than 7 kHz are resolvable. The signals were quite weak requiring an accumulation of 32 000 FIDs for the measurement of the weakest lines.

Conclusions

In summary, based on experimental proof intertwined with extensive theoretical characterization, we have shown for the first time, that ammonia forms a $lp \cdots \pi$ -hole interaction both with C_6F_6 and C_5F_5N and that this interaction, mainly established through electrostatic and dispersive forces, is slightly stronger than that of water due to the perfect alignment of the lone pair of ammonia with the π -hole. Nevertheless, the distances between the two moieties in the complexes are larger for ammonia demonstrating that the final geometry is a delicate balance between the different driving forces leading to the formation of the complex. Moreover, the barriers to rotation are smaller for the ammonia complexes with respect to those of water; thus we can conclude that the ammonia ligand produces stronger and more flexible interactions with respect to water both with C_6F_6 and C_5F_5N . Considering the two complexes formed by ammonia with C_6F_6 and C_5F_5N , we can assert that the insertion of a nitrogen in the ring (C_5F_5N) produces an increment of the binding energy (3–4 kJ mol^{−1}) and an increment in the height of the rotation barrier due to the additional interaction with the heterocyclic atom. We believe that these results can be considered relevant and helpful for the understanding of this particular kind of interaction, which seem to be increasingly fundamental in the study of materials, drugs, and proteins, as well as in the design of specific ligands.

Author contributions

W. Li: data curation, formal analysis, investigation, writing – review and editing; I. Usabiaga: data curation, formal analysis, investigation, visualization, writing – review and editing; C. Calabrese: conceptualization, data curation, formal analysis, investigation, visualization, validation, writing – original draft, writing – review and editing; L. Evangelisti: conceptualization, formal analysis, investigation, validation, writing – review and editing, funding acquisition; A. Maris: conceptualization, investigation, validation, and writing – review and editing, funding acquisition; L. B. Favero: formal analysis, and writing – review and editing; S. Melandri: conceptualization, funding acquisition, supervision, investigation, validation, visualization, writing – original draft, writing – review and editing.

Conflicts of interest

There are no conflicts to declare.

Acknowledgements

We acknowledge the CINECA award under the ISCRA initiative, for the availability of high-performance computing resources

and support. CC acknowledges the Spanish Government for a "Juan de la Cierva" contract and MICINN Ministerio de Ciencia e Innovación. W. L. thanks the China Scholarship Council (CSC) for financial support. This work was supported by the Italian MIUR (Attività Base di Ricerca), the University of Bologna (Ricerca Fondamentale Orientata) and Fondazione Cassa di Risparmio in Bologna.

Notes and references

- 1 P. Hobza and J. Řezáč, *Chem. Rev.*, 2016, **116**, 4911–4912.
- 2 H.-J. Schneider, *Angew. Chem., Int. Ed.*, 2009, **48**, 3924–3977.
- 3 E. Persch, O. Dumele and F. Diederich, *Angew. Chem., Int. Ed.*, 2015, **54**, 3290–3327.
- 4 I. Alkorta and S. J. Grabowski, *Comput. Theor. Chem.*, 2012, **998**, 1.
- 5 E. Arunan, G. R. Desiraju, R. A. Klein, J. Sadlej, S. Scheiner, I. Alkorta, D. C. Clary, R. H. Crabtree, J. J. Dannenberg, P. Hobza, H. G. Kjaergaard, A. C. Legon, B. Mennucci and D. J. Nesbitt, *Pure Appl. Chem.*, 2011, **83**, 1619–1636.
- 6 E. Arunan, G. R. Desiraju, R. A. Klein, J. Sadlej, S. Scheiner, I. Alkorta, D. C. Clary, R. H. Crabtree, J. J. Dannenberg, P. Hobza, H. G. Kjaergaard, A. C. Legon, B. Mennucci and D. J. Nesbitt, *Pure Appl. Chem.*, 2011, **83**, 1637–1641.
- 7 S. Scheiner, *Hydrogen Bonding*, Oxford University Press, New York, 1997.
- 8 P. Politzer, J. S. Murray and T. Clark, *Phys. Chem. Chem. Phys.*, 2010, **12**, 7748–7757.
- 9 J. S. Murray, P. Lane, T. Clark, K. E. Riley and P. Politzer, *J. Mol. Model.*, 2012, **18**, 541–548.
- 10 A. Bauzá, T. J. Mooibroek and A. Frontera, *ChemPhysChem*, 2015, **16**, 2496–2517.
- 11 R. Berger, G. Resnati, P. Metrangolo, E. Weber and J. Hulliger, *Chem. Soc. Rev.*, 2011, **40**, 3496–3508.
- 12 K. Müller, C. Faeh and F. Diederich, *Science*, 2007, **317**, 1881–1886.
- 13 M. Cametti, B. Crousse, P. Metrangolo, R. Milani and G. Resnati, *Chem. Soc. Rev.*, 2012, **41**, 31–42.
- 14 E. N. G. Marsh, *Acc. Chem. Res.*, 2014, **47**, 2878–2886.
- 15 A. A. Berger, J.-S. Völler, N. Budisa and B. Kocsch, *Acc. Chem. Res.*, 2017, **50**, 2093–2103.
- 16 K. Reichenbacher, H. I. Süss and J. Hulliger, *Chem. Soc. Rev.*, 2005, **34**, 22–30.
- 17 Q. Gou, L. Spada, Y. Geboes, W. A. Herrebout, S. Melandri and W. Caminati, *Phys. Chem. Chem. Phys.*, 2015, **17**, 7694–7698.
- 18 L. Spada, Q. Gou, Y. Geboes, W. A. Herrebout, S. Melandri and W. Caminati, *J. Phys. Chem. A*, 2016, **120**, 4939–4943.
- 19 R. J. Burns, I. K. Mati, K. B. Muchowska, C. Adam and S. L. Cockroft, *Angew. Chem., Int. Ed.*, 2020, **59**, 16717–16724.
- 20 L. M. Salonen, M. Ellermann and F. Diederich, *Angew. Chem., Int. Ed.*, 2011, **50**, 4808–4842.
- 21 R. Sanchez, B. M. Giuliano, S. Melandri, L. B. Favero and W. Caminati, *J. Am. Chem. Soc.*, 2007, **129**, 6287–6290.
- 22 W. Li, A. Vigorito, C. Calabrese, L. Evangelisti, L. B. Favero, A. Maris and S. Melandri, *J. Mol. Spectrosc.*, 2017, **337**, 3–8.
- 23 B. Velino, S. Melandri and W. Caminati, *J. Phys. Chem. A*, 2004, **108**, 4224–4227.
- 24 C. Calabrese, W. Li, G. Prampolini, L. Evangelisti, I. Uriarte, I. Cacelli, S. Melandri and E. J. Cocinero, *Angew. Chem., Int. Ed.*, 2019, **58**, 8437–8442.
- 25 L. Evangelisti, K. Brendel, H. Mäder, W. Caminati and S. Melandri, *Angew. Chem., Int. Ed.*, 2017, **56**, 13699–13703.
- 26 C. Calabrese, Q. Gou, A. Maris, W. Caminati and S. Melandri, *J. Phys. Chem. Lett.*, 2016, **7**, 1513–1517.
- 27 P. Halder, M. S. Krishnan and E. Arunan, *J. Mol. Spectrosc.*, 2020, **370**, 111277.
- 28 R. B. Mackenzie, C. T. Dewberry, R. D. Cornelius, C. J. Smith and K. R. Leopold, *J. Phys. Chem. A*, 2017, **121**, 855–860.
- 29 H. Wang, W. Wang and W. J. Jin, *Chem. Rev.*, 2016, **116**, 5072–5104.
- 30 K. Brendel, H. Mäder, Y. Xu and W. Jäger, *J. Mol. Spectrosc.*, 2011, **268**, 47–52.
- 31 Q. Gou, L. Spada, M. Vallejo-Lopez, S. Melandri, A. Lesarri, E. J. Cocinero and W. Caminati, *ChemistrySelect*, 2016, **1**, 1273–1277.
- 32 C. Calabrese, Q. Gou, L. Spada, A. Maris, W. Caminati and S. Melandri, *J. Phys. Chem. A*, 2016, **120**, 5163–5168.
- 33 S. Melandri, C. Calabrese, A. Maris, L. Evangelisti, W. Li and I. Usabiaga, *74th International Symposium on Molecular Spectroscopy*, Urbana-Champaign, IL, 2018.
- 34 D. D. Nelson Jr., G. T. Fraser and W. Klemperer, *Science*, 1987, **238**, 1670–1674.
- 35 B. M. Giuliano, S. Melandri, A. Maris, L. B. Favero and W. Caminati, *Angew. Chem., Int. Ed.*, 2009, **48**, 1102–1105.
- 36 S. Melandri, A. Maris and L. B. Favero, *Mol. Phys.*, 2010, **108**, 2219–2223.
- 37 B. M. Giuliano, A. Maris, S. Melandri and W. Caminati, *J. Phys. Chem. A*, 2009, **113**, 14277–14280.
- 38 D. A. Rodham, S. Suzuki, R. D. Suenram, F. J. Lovas, S. Dasgupta, W. A. Goddard III and G. A. Blake, *Nature*, 1993, **362**, 735–737.
- 39 L. Spada, N. Tasinato, F. Vazart, V. Barone, W. Caminati and C. Puzzarini, *Chem. – Eur. J.*, 2017, **23**, 4876–4883.
- 40 M. J. Frisch, G. W. Trucks, H. B. Schlegel and E. Al, *Gaussian 16, Revis. B.01*, 2016.
- 41 M. Juanes, I. Usabiaga, I. León, L. Evangelisti, J. A. Fernández and A. Lesarri, *Angew. Chem., Int. Ed.*, 2020, **59**, 14081–14085.
- 42 G. T. Fraser, F. J. Lovas, R. D. Suenram, D. D. Nelson and W. Klemperer, *J. Chem. Phys.*, 1986, **84**, 5983–5988.
- 43 W. Gordy and R. L. Cook, *Microwave Molecular Spectra*, New York, 1984.
- 44 M. D. Marshall and J. S. Muentner, *J. Mol. Spectrosc.*, 1981, **85**, 322–326.
- 45 X. Liu and Y. Xu, *Phys. Chem. Chem. Phys.*, 2011, **13**, 14235–14242.
- 46 J. Thomas, I. Pena, C. D. Carlson, Y. Yang, W. Jager and Y. Xu, *Phys. Chem. Chem. Phys.*, 2020, **22**, 23019–23027.
- 47 H. M. Pickett, *J. Mol. Spectrosc.*, 1991, **148**, 371.

- 48 J. K. G. Watson, *Vibrational Spectra and Structure*, Elsevier Science Publishers B.V., Oxford, New York, 1977.
- 49 J. Kraitichman, *Am. J. Phys.*, 1953, **21**, 17.
- 50 T. Lu and F. Chen, *J. Comput. Chem.*, 2012, **33**, 580–592.
- 51 R. F. W. Bader, *Atoms in Molecules: a Quantum Theory*, Oxford University Press, 1990.
- 52 E. R. Johnson, S. Keinan, P. Mori-Sánchez, J. Contreras-García, A. J. Cohen and W. Yang, *J. Am. Chem. Soc.*, 2010, **132**, 6498–6506.
- 53 J. Contreras-García, R. A. Boto, F. Izquierdo-Ruiz, I. Reva, T. Woller and M. Alonso, *Theor. Chem. Acc.*, 2016, **135**, 242.
- 54 B. Jeziorski, R. Moszynski and K. Szalewicz, *Chem. Rev.*, 1994, **94**, 1887–1930.
- 55 R. M. Parrish, L. A. Burns, D. G. A. Smith, A. C. Simmonett, A. E. DePrince III, E. G. Hohenstein, U. Bozkaya, A. Y. Sokolov, R. Di Remigio, R. M. Richard, J. F. Gonthier, A. M. James, H. R. McAlexander, A. Kumar, M. Saitow, X. Wang, B. P. Pritchard, V. Prakash, H. F. Schaefer III, K. Patkowski, R. A. King, E. F. Valeev, F. A. Evangelista, J. M. Turney, T. D. Crawford and C. D. Sherrill, *J. Chem. Theory Comput.*, 2017, **13**, 3185–3197.
- 56 S. Melandri, *Phys. Chem. Chem. Phys.*, 2011, **13**, 13901–13911.
- 57 J. U. Grabow, W. Stahl and H. Dreizler, *Rev. Sci. Instrum.*, 1996, **67**, 4072–4084.
- 58 T. J. Balle and W. H. Flygare, *Rev. Sci. Instrum.*, 1981, **52**, 33.
- 59 W. Caminati, A. Millemaggi, J. L. Alonso, A. Lesarri, J. C. Lopez and S. Mata, *Chem. Phys. Lett.*, 2004, **392**, 1–6.
- 60 W. Caminati, L. Evangelisti, G. Feng, B. M. Giuliano, Q. Gou, S. Melandri and J.-U. Grabow, *Phys. Chem. Chem. Phys.*, 2016, **18**, 17851–17855.